Versatile wet deposition techniques for functional oxide coatings

M.A. Aegerter *, J. Puetz, G. Gasparro, N. Al-Dahoudi

Department of Coating Technology, Leibniz—Institute for New Materials (INM), Im Stadtwald, Gebaeude 43, D-66123 Saarbruecken, Germany

---

Abstract

Functional oxide coatings are essential components in a variety of today's technical products and developments, but often applications are limited by the low flexibility and the high cost of the vapor phase deposition techniques used at present. Wet chemical processes based on the sol–gel and nanoparticle approaches can provide desired alternatives for a large number of such applications. This is shown for the high temperature sol–gel processing and the low-temperature nanoparticle approach with a focus on transparent conducting oxides (TCO). The paper presents recent developments realized at the Institute for New Materials (INM) in the field of thin film deposition including the inside coating of cavities such as tubes in optical quality using a modified dip coating equipment as well as the coating of complex shaped substrates and the high-throughput coating of large area flat glasses using a spray technology. Moreover the use of functional crystalline nanoparticles allows now to apply thick coatings or patterns with elaborate functionalities on temperature sensitive substrates like plastics and pre-shaped glass parts by UV-curing at low temperature. The concept is exemplified for transparent conducting ITO coatings.

Keywords: Sol–gel; Dip coating; Spray process; Nanoparticles; Transparent conducting coatings

---

1. Introduction

The coating of glass surfaces with transparent thin films allows the tailor-made functionalization retaining to a large extent the advantages of the approved substrate material. The wet chemical sol–gel coating has to date asserted its position along with the established vacuum processes, last but not least because of the low cost and the high coating quality. Thus, especially antireflection systems and color effect filters on the basis of SiO_2 and TiO_2 are deposited on large area flat glass using the dip coating process.

A strong argument for the employment of wet chemical processes is found in the higher flexibility regarding the geometry and the number of substrates to be coated or the process control, as for example, the curing method. Generally, this can be accomplished either by an adaptation of the coating lacquer and the chosen coating process or an adjustment of the equipment/set-up to the requirements of the respective substrate form or the application profiles.

The paper describes some successful implementations on glass and plastic substrates that have been achieved with transparent conducting oxide coatings (TCO). The next section describes a modified dip coating process developed to coat the inner side of cavities. This is followed by a discussion of the requirements concerning the sol composition in order to deposit TCO coatings using a spraying process at room temperature. The last section reports the development of nanocomposite sols made with crystalline conducting nanoparticles, which allows to coat heat sensitive substrates like plastics by UV-curing.

2. Modified dip coating

The dip coating process is generally characterized by a high optical quality and a homogeneous thickness of the deposited coatings [1]. It is, however, difficult to obtain uniform film thickness on shaped substrates and in particular inside cavities, as here the formation of the film is negatively influenced by a change of the flow behavior as well as limited drying inside. The obtained coatings often do not comply with the quality requirements of optical and electrical applications in respect of homogeneity and reproducibility.

---

* Corresponding author. Tel.: +49-681-9300-317; fax: +49-681-9300-249.

E-mail address: aegerter@inm-gmbh.de (M.A. Aegerter).

For coating at inner sides of tubes with a film of high optical quality, the conventional dip coating process had to be modified in order to achieve an enforced laminar flow inside the tubes [2–4]. This was realized by introducing an additional exhausting glass pipe (5 mm outer diameter) that was put in the solution vessel and introduced from below into the tube with the internal end placed just above the coating solution (Fig. 1). The external end of the exhausting pipe was connected to a diaphragm pump with an adjustable pulsation-free flow of air of up to 210 l/h (Fig. 1). The flow rate that is necessary to obtain homogeneous films depends on both the withdrawal speed and the inner diameter of the tube. For the two tubes used in these experiments with outer diameters of 14 and 50 mm a constant flow of 50 and 210 l/h respectively was generated.

Compared to the coating of flat substrates, however, it is also necessary to modify the sequence of the dip coating process. For the formation of an internal laminar flow it is important to have a tube that is closed up on the lower end (which is the case as long as the tube is dipped into the solution). Otherwise, the internal flow would come to an end leading to inhomogeneous films. Therefore the tube is not completely withdrawn, but is kept in the solution just enough to seal the tube at the lower end. After a drying time of 1 min the tube is then withdrawn completely from the solution and the adhering solution is wiped off. The films prepared in this manner were then dried and heat treated as usual.

Without this procedure the optical quality, the uniformity and the morphology of the coatings (both inside and outside the tubes) are not satisfying [2–4]. The bad coating quality seems to originate from a saturation of the inside of the tube with the solvent vapor, which consequently leads to a restricted and delayed drying of the deposited wet film as shown by images of an IR thermocamera availing the evaporation cooling (Fig. 2). For the initial drying and hydrolysis during the sol–gel dip coating, the flow of the air in the surroundings of the film is extremely important and decisively influences the properties of the resulting coating. As the solvent vapors are usually specifically heavier than the ambient atmosphere, they start sinking downwards and generate a constant laminar flow over the film surface. This increases the evaporation rate by reducing the partial pressure of solvent next to the surface and keeps the concentration of water constant by permanently renewing the atmosphere. To obtain a uniform thickness this flow has to be laminar and thus should be protected against external influences like draft and convection more should be reproducible.

The additional exhausting pipe allows to generate a continuous flow of the air through the substrate which not only guarantees the removal of the evaporated solvent (keeping the evaporation rate high) but also the supply of water that is required for the hydrolysis of the sol–gel wet film. The resulting flow conditions are thus comparable to those on the outer side of the tube.

The morphology of the coatings obtained by both procedures is shown in Fig. 3 and reflects the different drying behavior mentioned above. While the morphology of the coatings made by a conventional procedure is irregular with many cracks, the surface of coatings

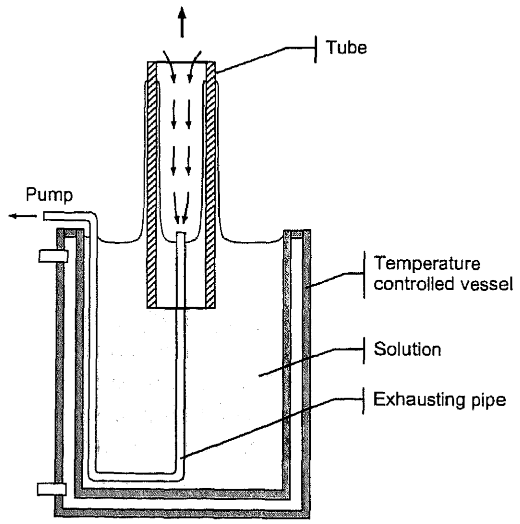

Fig. 1. Experimental set-up for the dip coating of tubes under forced flow conditions with an internal exhausting pipe tube and a temperature controlled vessel.

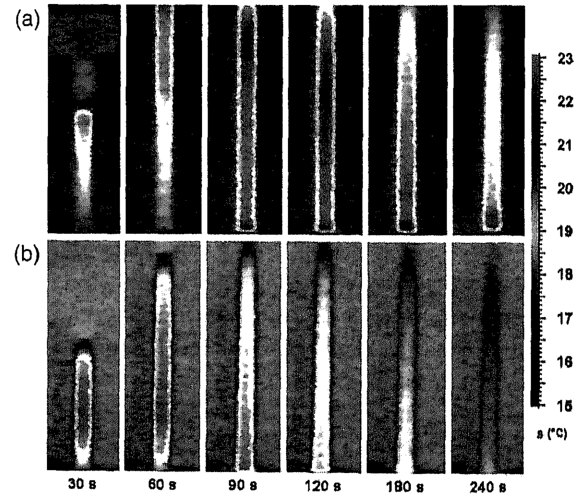

Fig. 2. Thermographic images of the withdrawal process during dip coating of a glass tube (30 cm long, 1.1 cm Ø) with ethanol (4 mm/s). The background temperature is 21 °C. Top: Conventional procedure showing an inhomogeneous temperature repartition caused by a delayed and restricted drying inside the tubes. The lowest temperature reached is about 16.5 °C (upper part at 90 s, middle part at 120 s, lower part at 180 s). Bottom: Dip coating under formed flow condition with the addition of an exhausting pipe. The temperature repartition is homogeneous and the lowest temperature reached is only 18 °C (30 and 60 s). The tube temperature practically returns to that of the background after 240 s.

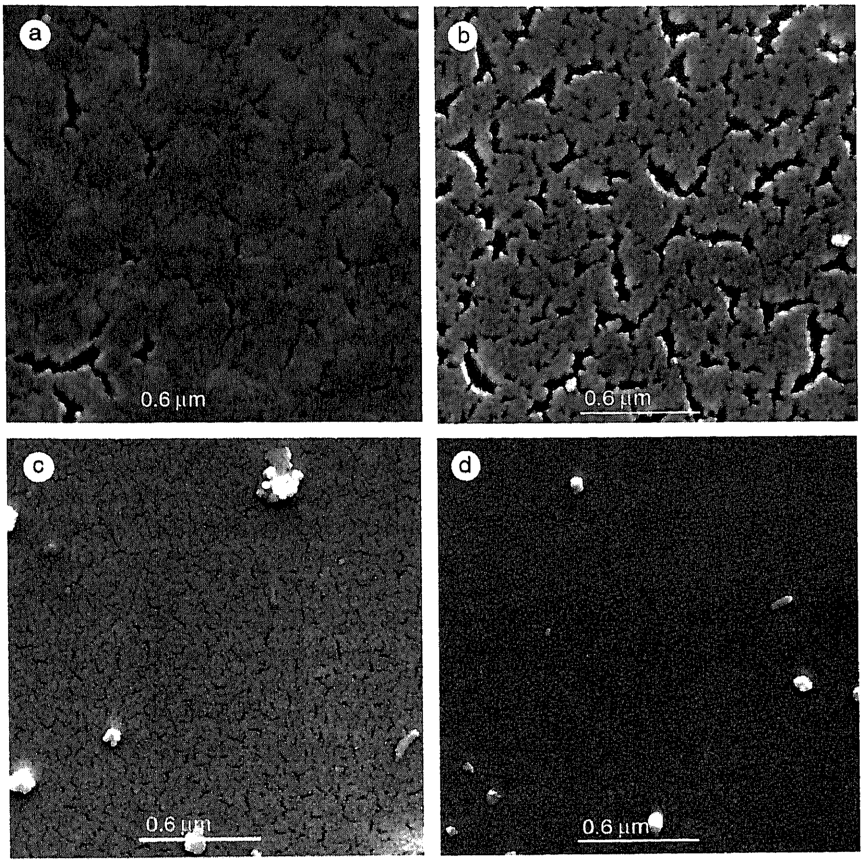

Fig. 3. Morphology of ATO coatings represented by SEM (selected area: 2.1 × 2.1 μm^2) of conventionally dip coated tubes ((a) outer and (b) inner coating) and tubes coated under forced flow conditions ((c) outer and (d) inner coating).

prepared with the modified equipment is smooth (especially the inner coating which is crack-free on this scale and almost fully dense). This clearly shows that the inside flow control is even more effective than the intrinsic flow on the outside.

This new procedure is applicable to any type of conventional sol–gel coating material. The thickness uniformity can now be used to built up interference systems from oxide materials like SiO_2 and TiO_2 for light selection. Transparent conducting ATO coatings obtained with this modified dip coating system and exemplified in this paper present a specific resistivity similar to that obtained with flat substrates using the same sol, about 2×10^{-2} Ω cm and can be used in applications where a moderate conductivity is sufficient, e.g. for antistatic purposes (Fig. 4).

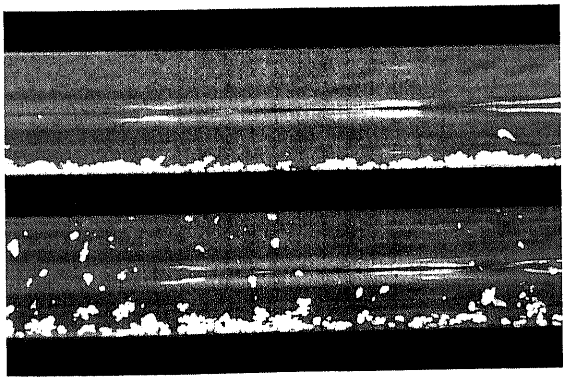

Fig. 4. Photograph of an ATO antistatic-coated (top, $R_\square \approx 3$ k$\Omega_\square$) and an uncoated borosilicate glass tube (bottom) with polystyrene beads. Tube diameter: 40 mm.

3. Spray coating

A further flexibility of the film deposition can be obtained by the utilization of the spray process for the sol–gel systems. This technique exhibits fundamental advantages (if a high thickness uniformity is not required):

- higher speed of deposition,
- higher flexibility in the shape of the substrate,
- lower total amount of coating solution to have in stock,
- reduced aging and contamination of the coating solution,
- availability of the spraying equipment.

In this case, the modification of the coating solution is decisive in order to cope with the peculiarities of the film formation during spraying. Coating solutions for sol–gel dip coating are usually based on low boiling point solvents like ethanol or 2-propanol in order to guarantee a fast and complete solvent evaporation in the initial stages of withdrawal. If such solutions are used for a spray deposition, the resulting coating quality is not satisfying. As most of the solvent already evaporates during the flight phase, an almost dry powder hits the substrates and the liquid mobility is not sufficient to level out and form a homogeneous coating.

The problem can easily be overcome by the addition of solvents with lower evaporation rates which is a basic concept for the control of film formation of paints and lacquers [5]. The approach is also suitable for the much thinner sol–gel films as the early processes of film formation are similar in both cases. The evaporation rate depends on a variety of parameters and environmental conditions so that an empirical treatment is more or less unavoidable. A good approximation for the evaporation rate, however, is given by the boiling point of the solvent, as its volatility generally decreases with increasing boiling point within a group of chemically related solvents. But, besides the evaporation rate, solvent properties like the substrate wetting and interactions with the sol–gel precursors are also decisive, so that mainly glycols and glycol ethers are used as additives.

The feasibility of this concept has already been shown earlier for $PbO–SiO_2$ coatings containing Au colloids [6] as well as for SiO_2, TiO_2, ATO and ITO [7,8]. In all these cases high boiling point solvents [9,10] (like glycols or glycol ethers) were successfully used to obtain homogeneous films.

One of the advantages of the spray coating process is the significantly higher coating speed for thin films compared to the dip coating process, which can be realized on flat substrates with the help of automated equipment. However, normally the film homogeneity is lower. Nevertheless, satisfying optical properties were obtained for transparent conducting coatings (ATO) up to a size of 20×30 cm^2 (Fig. 5) with a surface resistivity in the lower k$\Omega_\square$ range and a deviation of only ±2 k$\Omega_\square$ [5].

The spray coating process also has advantages when it comes to the coating of shaped bodies as it is depicted in Fig. 6 for a large tube with flange fittings. The antistatic ATO coating, which has been sprayed on manually, is optically homogeneous and has a resistance of merely 30–40 kΩ across the entire height of 46 cm. It can be emphasized that it was also allowed to provide the side flanges with antistatic properties. The coatings which were heated at 550 °C are characterized by a high mechanical and chemical stability due to the SnO_2-based coating material.

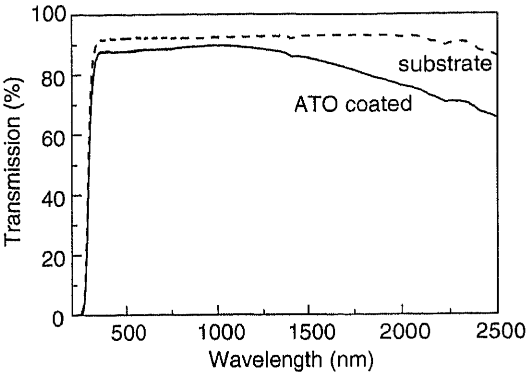

Fig. 5. Optical transmission spectra of a spray deposited sol–gel ATO sample (80 nm thick, $R_\square \approx 4$ k$\Omega_\square$) (solid) and the borosilicate glass substrate (dashed).

Fig. 6. Manually spray deposited antistatic sol–gel ATO coating on the outer side of a large tube with flange fittings (46 cm height, 22 cm ∅). The resistance measured over the length of the tube is 30–40 kΩ.

4. Transparent conducting nanocomposite coatings

The basic idea of nanocomposite materials involves the development of hybrid organic–inorganic sols containing the highest possible amount of already crystalline oxide nanoparticles. The major advantages of this technique are the separation of the crystallization step of the material from the process of film formation, the redispersability of the obtained nanoparticles in a variety of lacquer composition, the possibility of obtaining thick single coatings (>500 nm) and the low light scattering level of the coatings due to the low size of the particles (<30 nm) assuring a high optical transmission. An example of application is given here for transparent conducting ITO coatings.

The preparation of crystalline conducting ITO nanoparticles has already been described in detail in previous papers [11–14]. Redispersible powders so far achieved have an average grain size up to 25 nm, a density of 6.67 g/cm^3 (about 95% of the theoretical density of 7.0 g/m^3) and blue color, indicating that they are conducting. These powders can be fully redispersed in ethylene glycol using a carboxylic acid as dispersing agent with solid contents up to 80 wt%. The paste is stable for several months without evidence of precipitation if a pH < 6 is maintained.

A sol adequate for obtaining conducting single layer coatings with a thickness up to 1 μm on glass is obtained by diluting the paste in ethanol [15]. The properties of such coatings after a high temperature sintering ($550 < T < 1000$ °C) are reported elsewhere [15–17].

The use of polymerisable organic additives offers the possibility to cure the layers by UV irradiation at low temperature allowing to coat any heat-sensitive substrate (plastics, preshaped glasses, etc.). A high content of nanoparticles in the sol, in combination with an adequate amount of organic binder, guarantees a reasonable conductivity and good mechanical resistance and also favors the generation of thick single coatings.

Among the different additives which have been tested [17], the use of 3-methacryloxypropyltrimethoxysilane (MPTS) gave the best electrical, optical, structural and mechanical properties.

The lowest resistivity, $\rho = 4.5 \times 10^{-2}$ Ωcm, was obtained for coatings made with a sol containing 6 vol.% MPTS, polymerized during 2 min under a 105 mW/cm^2 UV irradiation (Beltron) followed by a heat treatment at 130 °C during 2 h in the air and annealing in N_2 or forming gas (N_2/H_2) atmosphere at 130 °C during 30 min. However, this state is only stable if the coatings are kept in vacuum or inert atmosphere, whereas the sheet resistance increases slightly to a stable value of 1.7 kΩ$_\square$ ($\rho = 9.5 \times 10^{-2}$ Ωcm) after seven days in the air. This variation is reversible if the sample is again exposed to UV light. It occurs essentially due to the variation of the carrier density N and not the mobility μ (Fig. 7). The ratio ρ (seven days)/ρ (initial) depends on the thickness of the coating and equals typically 10 for a 100-nm-thick coating and diminishes to a value of 2 for a coating of 1 μm thickness.

The surface properties of the coatings are also reversibly altered during the UV treatment and the storage in the air. Fig. 8 shows the evolution of the electron work function ϕ, measured using a Kelvin probe, and the surface energy calculated from the measurements of the contact angle using different liquids. UV irradiation decreases the work function from 5.3 to 4.9 eV, while the surface energy increases from 30 to 75 mN/m. The variation of this latter property is essentially due to its polar component (σ_p) as the dispersed ones remain unaffected. When the coatings are stored in a protective atmosphere, both properties remain constant but they return to their original values when the coatings are stored in air. As both properties reflect a surface effect, the values are fully correlated.

The exact nature of these reversible variations is not yet clear but it should involve oxygen species interacting with the particle's surface. They probably act as electron traps and are likely released by the UV irradiation. The creation of electron–hole by the UV irradiation followed by a redox reaction at the particle surface is not excluded. When the coatings are kept in air, oxygen molecules from the atmosphere diffuse back into the still porous coating.

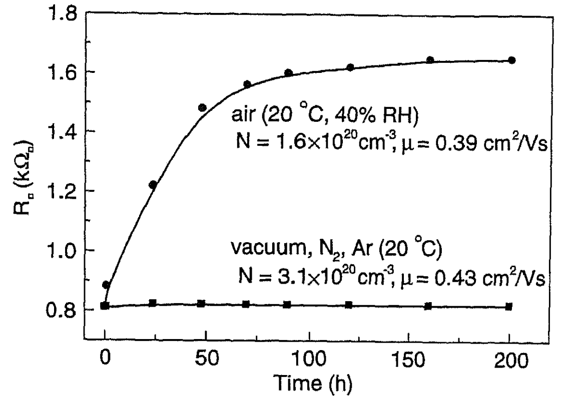

Fig. 7. Time evolution of the resistivity of MPTS/ITO nanocomposite coatings (570 nm thick) kept in an inert atmosphere (vacuum, Ar, N_2) and in air respectively. The coatings have been UV irradiated and then post annealed in a reducing atmosphere. The values of the carrier concentration N and mobility μ were measured after a 200 h storage time.

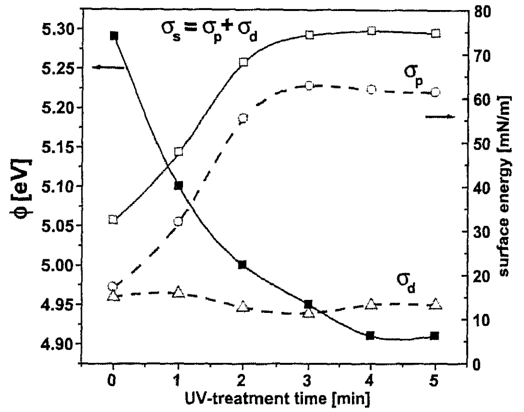

Fig. 8. Variation of the electron work function ϕ and surface energy σ of a nanocomposite MPTS/ITO coating during UV irradiation (105 mW/cm^2). The indices p and d stay for the polar and dispersed components respectively.

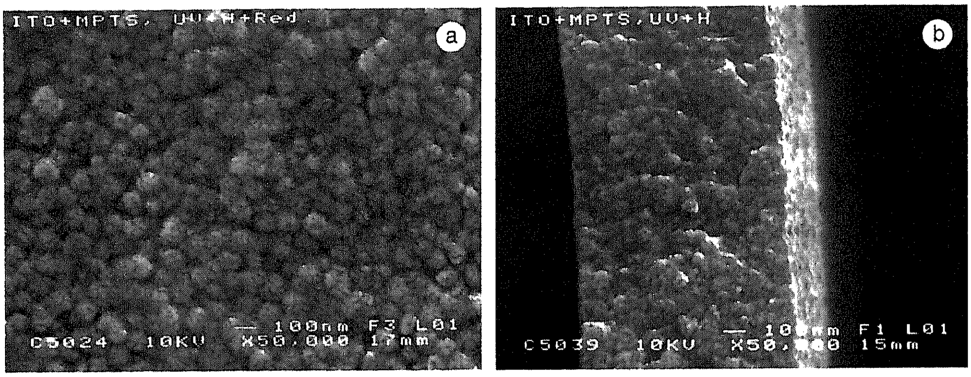

Fig. 9. Morphology of a MPTS/ITO nanocomposite coating. SEM images of (a) coating surface, (b) coating cross-section.

The surface morphology of the coatings observed by SEM (Fig. 9) consists of loosely packed globular grains (raspberry like) with a size of about 100 nm formed by the aggregation of the ITO nanoparticles and linked together by a small strip of polymerized MPTS. The coating roughness measured by white light interferometry (WLI) on a 53×70 μm^2 area with a lateral resolution of 0.6 μm is $R_a = 0.85$ nm, with a peak-to-valley maximum value of $R_{PV} = 15$ nm. When measured with a higher resolution on a 1×1 μm^2 area by atomic force microscopy (AFM), the values are $R_a = 4$ nm and $R_{PV} = 28$ nm.

The optical transmission and reflection of a coating deposited on a polycarbonate (PC) substrate is shown in Fig. 10, giving transmission of more than 85% in the visible range. The influence of the charge carriers is clearly seen by the strong absorption ($A = 1 - T - R$) occurring in the near IR range ($800 < \lambda < 3$ μm) and the increase of the reflection starting at $\lambda \approx 1.7$ μm with a value up to $R \approx 40\%$ at $\lambda = 20$ μm (Fig. 10b). Similar results have been obtained for coatings deposited on different plastic material such as polymethylmethacrylate (PMMA), polyethyleneterephthalate (PET), polyvinyl chloride (PVC) either on thick substrates (up to 10 mm) or on foils ($\geqslant 0.2$ mm). The strong decrease of the transmission in the UV range ($\lambda < 400$ nm) due to ITO band-band transition makes these coatings interesting for protection of plastic substrates against UV radiation, while the strong decrease of the transmission due

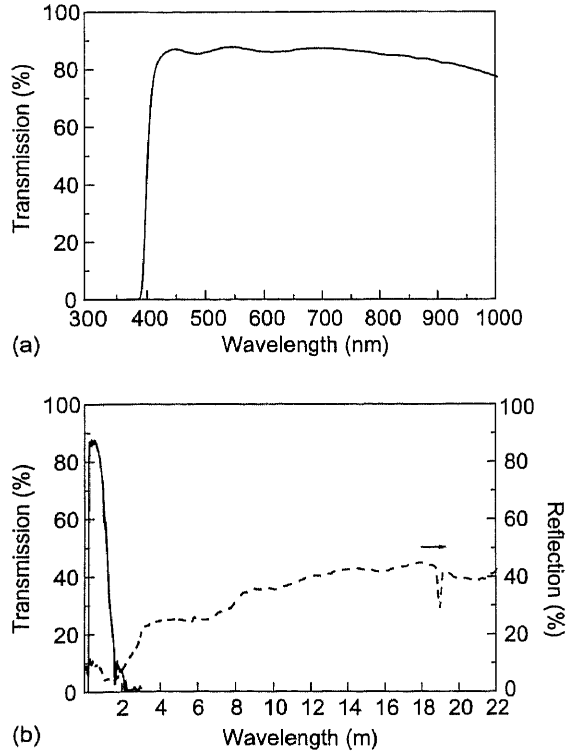

Fig. 10. Optical spectra of an MPTS/ITO nanocomposite coating deposited on a polycarbonate (PC) substrate in the visible range and NIR (a) and the far IR (b). The coating has been UV treated and annealed in forming gas.

Table 1
Mechanical properties of MPTS/ITO nanocomposite coatings deposited on polycarbonate substrates

Test	Classification
Adhesion	
Tape test[a]	Passed
Lattice cut test[b]	Gt0
Abrasion	
Cotton cloth[c]	Class 1
Hard rubber[d]	Class 1
Taber test[e]	Haze 15% at 10 cycles, 42% at 1000 cycles
Hardness	
Pencil test[f]	1 H

[a] DIN 58196-K2.
[b] ASTM 3359, DIN 53151.
[c] DIN 58196-H25.
[d] DIN 58196-G10.
[e] DIN 52347/CS10F/5,4N.
[f] ASTM 3363-92a.

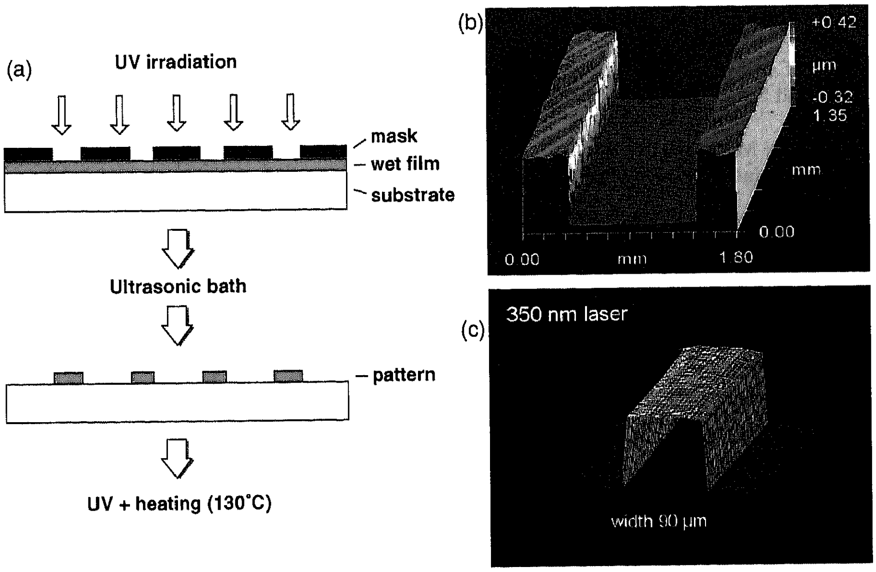

Fig. 11. Line patterns obtained by selective irradiation through a mask (a, b) or by direct irradiation with a 350 nm laser (c) in combination with a removal of the non-exposed area by washing.

to the carrier absorption observed at $\lambda > 900$ nm offers the heat radiation protection.

The mechanical properties of the coatings deposited on PC substrates have been characterized by various standard tests (Table 1). The adhesion is in agreement with the tape test procedure (DIN 58196-K2) and the lattice cut test (ASTMD 3359, DIN 53151-Gt0 completely smooth cutting edges). No scratch was observed after 10 rubbing cycles with an eraser under a load of 10 N (class 1 DIN 58196-G10) as well as with the milder rubbing with a cotton cloth (25 cycles, DIN 58196-H25). But the results of the Taber test show that the coatings cannot be classed as really hard materials, which is confirmed by a hardness of 1 H obtained from the pencil test ASTM D 3363-92a. Higher values are however obtained when the amount of MPTS is increased, but such coatings present also a higher sheet resistance.

In addition, antiglare-antistatic coatings have been deposited successfully by a spraying process resulting in a final surface morphology with micrometer size roughness [17,18].

The coatings are also easily patterned by selective UV irradiation. The exposed parts strongly adhere to the substrate, whereas the non-exposed parts are easily washed in ethanol with the aid of ultrasound (Fig. 11a). Typical line patterns obtained by such a UV irradiation through a metallic mask placed directly on top of the wet coating and by 350 nm laser irradiation are shown in Fig. 11b and c respectively.

5. Conclusions

A versatile sol–gel coating technology was developed to deposit oxide films in a cost-efficient way. The spectrum of functional coatings ranges from optical filters, through improvement of mechanical properties to transparent conducting coatings for sophisticated electronic and antistatic applications. Different requirements, which are introduced by substrates or applications, can normally be allowed for by adjustments of the coating solution as well as a modification of the coating process—building up on the rich experience of wet coating. In this way, optical films can be deposited with the desired flexibility on a variety of substrate shapes and materials.

References

[1] P.R. Schunk, A.J. Hurd, C.J. Brinker, in: S.F. Kistler, P.M. Schweizer (Eds.), Liquid Film Coating, Chapman & Hall, London, 1997, p. 672.

[2] F.N. Chalvet, Nasschemische Aufbringung von transparenten leitfähigen ATO-Schichten in Rohren, Diploma Thesis, EEIGM (Nancy) and Institut fuer Neue Materialien—INM, Saarbruecken, Germany, 2002.

[3] J. Puetz, F.N. Chalvet, M.A. Aegerter, in: E.J.A. Pope, H.K. Schmidt, B.S. Dunn, S. Shibata (Eds.), Sol–Gel Optics VI, Proc. of SPIE, vol. 4804, 2002, p. 73.

[4] J. Puetz, F.N. Chalvet, M.A. Aegerter, in: C.P. Klages, H.J. Glaeser, M.A. Aegerter (Eds.), Proceedings of the 4th ICCG—International Conference on Coatings on Glass, Braunschweig, Germany, 2002, p. 215. Thin Solid Films, in press.

[5] J. Puetz, G. Gasparro, M.A. Aegerter, in: C.P. Klages, H.J. Glaeser, M.A. Aegerter (Eds.), Proceedings of the 4th ICCG—International Conference on Coatings on Glass, Braunschweig, Germany, 2002, p. 179 and Thin Solid Films 442 (2003) 40.

[6] C. Fink-Straube, A, Kalleder, T. Koch, M. Mennig, DE Patent No. 19840525 A1, 9 March 2000.

[7] C. Löser, C. Rüssel, Glass Sci. Technol. (Glasstech. Ber.) 73 (2000) 270.

[8] C. Löser, C. Rüssel, Glass Sci. Technol. (Glasstech. Ber.) 74 (2001) 106.
[9] J. Bielemann, Additives For Coatings, Wiley, Weinheim, 2001.
[10] D. Stoye, Paints, Coatings and Solvents, Wiley-VDH, Weinheim, 1993.
[11] N. Al-Dahoudi, M.A. Aegerter, Mater. Sci. 20 (2002) 71.
[12] D. Burgard, C. Goebbert, R. Nass, J. Sol–gel Sci. Technol. 13 (1998) 789.
[13] C. Goebbert, R. Nonninger, H. Schmidt, Verfahren zur Herstellung von Suspensionen, Pulvern und Formkörpern von Indium-Zinn-Oxid, DE 19840527 A1, 2000.
[14] C. Goebbert, M.A. Aegerter, D. Burgard, R. Naß, H. Schmidt, MRS Symp. Proc. 520 (1998) 293.
[15] C. Goebbert, M.A. Aegerter, D. Burgard, R. Naß, H. Schmidt, J. Mater. Chem. 9 (1999) 253.
[16] C. Goebbert, R. Nonninger, M.A. Aegerter, H. Schmidt, Thin Solid Films 351 (1998) 79.
[17] N. Al-Dahoudi, PhD Thesis, Universitaet des Saarlandes and Institut fuer Neue Materialien—INM, Saarbruecken, Germany, 2003.
[18] N. Al-Dahoudi, M.A. Aegerter, in: Coatings on Plastic Substrates, J. Sol–gel Sci. Technol. 27 (2003) 81 (special issue).